Forest-CEW Technical Documentation

Jiye ZENG

<zeng@nies.go.jp>

National Institute for Environmental Studies

Tsukuba, Ibaraki, 305-8506, Japan

Zeng Hong TAN

<tanzh@xtbg.ac.cn>

College for Ecology and Environmental Sciences, Hainan University

Hainan, Haikou 570228, China

April 2018

1 Introduction

This technical documentation focuses on the model structure and equations for ecosystem processes. Readers who are interested in the literature review concerning Forest-CEW should refer to Tan et al. (2018).

Forest-CEW comprises objects in a hierarchy structure (Figure 1). Plant and soil are the two types of tangible objects on the hierarchy top. A plant is made of foliage and stem. A foliage includes sunlit and shaded leaves. Soil has roots, which are consisted of fine and coarse roots. Although litter should be a tangible object on the hierarchy top, the implementations for its processes are included in foliage and stem as its decomposition rate depends on its origin.

Tree and shrub are plant with different properties.

Forest-CEW also includes intangible objects for handling processes related to rain water, radiation energy, and aerodynamics.

Using Forest-CEW requires these measurements above canopy: air temperature (Ta), vapor pressure deficit (VPD), wind speed (U), global solar ration (SR), downward long wave radiation (LR), precipitation (Prec), air pressure (P), and air CO2 concentration (CO2). It also requires two boundary conditions in the deep soil layer: temperature (Td) and water content (Wd).

For the convenience of discussion, we listed all symbols, their units and meanings in Table 1. When they are used in equations, we omit their definitions wherever possible. Subscripts of u, s, p, g, soi, ir, and vis may be attached to a symbol to indicate foliage or leaf, stem, plant, ground, soil, long wave radiation, and visible light radiation respectively. But they are often omitted when no confusion will be caused.

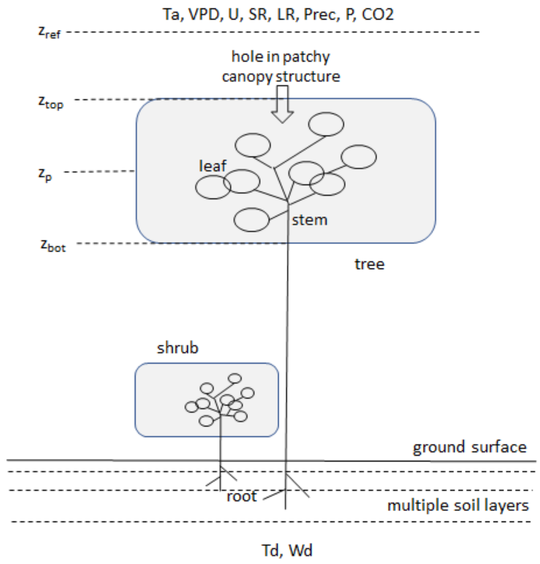

Figure 1. Conceptual illustration of a forest ecosystem.

2 Aerodynamics

The aerodynamic model computes the wind profile from canopy top to the ground and derive the conductance for heat and vapor fluxes from the profile. Following Campbell and Norman (1998), we define the zero-plane displacement (z_d); the roughness length scale for momentum (z_m), heat (z_h) and vapor (z_v); and the characteristic height of plant (z_p) as

$$z_d = 0.77 z_{top} \;, \tag{1}$$

$$z_m = 0.13 z_{top} \;, \tag{2}$$

$$z_h = z_v = 0.2 z_m \;, \tag{3}$$

$$z_p = z_m + z_d \;. \tag{4}$$

The stability indicator of the air inside the canopy is related to the sensible heat flux from z_p to the reference height z_{ref}, the air temperature T_p at z_p, and the friction velocity u^* above z_p, i.e.,

$$\xi = \frac{\kappa z_p H}{\rho c_p T_p u^{*3}} \;, \tag{5}$$

$$u^* = \frac{\kappa u_{ref}}{ln\left(\frac{z_{ref} - z_d}{z_m}\right) + \phi_M} \;. \tag{6}$$

The diabetic correction factor for momentum (ϕ_M) and heat (ϕ_H) Under stable condition ($\xi>0$) can be expressed as

$$\phi_M = \phi_H = 6 ln(1 + \xi) \tag{7}$$

and under unstable condition ($\xi<0$) as

$$\phi_H = -2 ln\left(\frac{1 + \sqrt{1 - 16\xi}}{2}\right) \;, \tag{8}$$

$$\phi_M = 0.6 \phi_H \;. \tag{9}$$

Having obtained u^*, ϕ_M and ϕ_H, the wind speed on top and inside of canopy can be estimated by

$$u_{top} = \frac{u^*}{\kappa}\left[ln\left(\frac{z_{ref} - z_d}{z_m}\right) + \phi_M\right] \;, \tag{10}$$

$$u(z) = u_{ref} exp\left[\sqrt{\frac{0.2 LAI z_{top}}{l_m}}\left(\frac{z}{z_{ref}} - 1\right)\right] \;, \tag{11}$$

$$l_m = \left(\frac{6 * d^2 z_{top}}{\pi LAI}\right)^{1/3} \;. \tag{12}$$

For a tree, the wind speed u_{ref} at z_{ref} is U, but a the shrub, z_{ref} is the bottom height of the tree foliage z_{bot} and $u_{ref}=u(z_{bot})$.

Finally, we can estimate the heat and vapor conductance between airs by

$$g_H = \frac{\kappa^2 u_p}{\left[ln\left(\frac{z_{ref}-z_d}{z_m}\right)+\phi_M\right]\left[ln\left(\frac{z_{ref}-z_d}{z_h}\right)+\phi_H\right]} , \quad (13)$$

$$g_V = 0.622 g_H \; ; \quad (14)$$

and the heat and vapor conductance between leaf or stem surface and air by

$$g_h = 0.135 \frac{m_a}{\rho} \sqrt{\frac{u_p}{d}} , \quad (15)$$

$$g_v = 0.147 \frac{m_w}{\rho_w} \sqrt{\frac{u_p}{d}} . \quad (16)$$

3 Energy

3.1 Visible radiation

The energy model of Forest-CEW is based on the idea of the two-sources model of Blyth et al. (1999). However, to distinguish the absorptions of visible radiation (VIS) by sunlit and shaded leaves, Forest-CEW divides the foliage into at least 10 layers to simulate VIS absorptions. The actual number of layers is determined by the condition that neither the leaf area index (LAI) nor the stem area index (SAI) in a layer is more than 0.1. This approach is similar to the method of the CANOAK model (Baldocchi and Harley, 1995; Baldocchi and Wilson, 2001).

The reflectivity and absorptivity of leaves in a layer are calculated by

$$\alpha' = \alpha \Delta L , \quad (17)$$

$$\beta' = \beta \Delta L , \quad (18)$$

where α and β are the reflectivity and absorptivity per unit LAI and ΔL is the LAI in a layer. Sunlit leaves in a layer absorb the transmitted downward VIS from above

$$I_{vis}(i) = \beta' I_{vis}^{\downarrow}(i) \quad (19)$$

and shaded leaves absorb reflected upward VIS

$$I_{vis}(i) = \beta' I_{vis}^{\uparrow}(i) , \quad (20)$$

where

$$I_{vis}^{\downarrow}(i) = (1 - \alpha' - \beta') I_{vis}^{\downarrow}(i-1) + \alpha' I_{vis}^{\uparrow}(i+1) , \quad (21)$$

$$I_{vis}^{\uparrow}(i) = (1 - \alpha' - \beta') I_{vis}^{\uparrow}(i-1) + \alpha' I_{vis}^{\downarrow}(i+1) . \quad (22)$$

The downward VIS above tree canopy is obtained from the global solar radiation by

$$I_{vis}^{\downarrow} = 0.46SR\ . \tag{23}$$

The reflected VIS by ground surface are calculated by its albedo and the transmitted VIS through tree or shrub:

$$I_{vis}^{\uparrow} = \alpha I_{vis}^{\downarrow}\ . \tag{24}$$

The total VIS absorption by foliage is the integrated VIS absorptions by sunlit and shaded leaves:

$$I_{vis} = \sum \beta' \left(I_{vis}^{\downarrow}(i) + I_{vis}^{\uparrow}(i) \right). \tag{25}$$

The VIS absorption by stem is calculate similarly. As plant is assumed to have a two-layer structure (to be discussed below), the order of calculating VIS absorption is foliage to stem for downward VIS and the reverse for upward VIS.

The absorbed VIS by ground surface are calculated by surface albedo and transmitted VIS through tree or shrub as

$$I_{vis} = (1 - \alpha) I_{vis}^{\downarrow}\ . \tag{26}$$

3.2 Long wave radiation

Forest-CEW follows the method of LSX model (Pollard and Thompson, 1995) for the absorption of long wave radiation (IR) as the method of Blyth et al. (1999) cannot separate the absorptions by foliage and stem. Again, our implementation is quite different as their methods incorrectly used the plant area index (PAI, the vertical projection area of canopy). In the method of Blyth et al. (1999), PAI was used to calculate the un-intercepted IR, but not in IR absorption by vegetation. As a result, the total absorption of sky IR by vegetation and soil is larger than sky IR itself; and the total net IR absorption is independent of soil temperature, which is valid only when PAI=1. In the method of Pollard and Thompson (1995), PAI was used to calculate the available downward IR for shrub and upward IR for tree, but was not considered the absorption equations.

Our implementation calculates the emissivity of foliage and stem by

$$\varepsilon_u = PAI \left(1 - e^{-0.5 f_{em} \frac{LAI}{\bar{\mu}}} \right), \tag{27}$$

$$\varepsilon_s = PAI \left(1 - e^{-0.5 f_{em} \frac{SAI}{\bar{\mu}}} \right). \tag{28}$$

Comparing with the method of the LSX model, one will notice that the equations include PAI to account for the effective LAI and SAI for IR absorptions. By doing so, Forest-CEW does not consider the direct transmit of IR through the patchy holes of a plant. The average inverse diffuse optical depth $\bar{\mu}$ was introduced in the two-stream radiation model of Dickinson (1983) and used in the SiB model (Sellers et al., 1986). It can be expressed as

$$\bar{\mu} = \frac{1}{\emptyset_2}\left\{1 - \frac{\emptyset_1}{\emptyset_2} ln\left(\frac{\emptyset_1+\emptyset_2}{\emptyset_1}\right)\right\}, \quad (29)$$

$$\emptyset_1 = 0.5 - 0.633\chi - 0.33\chi^2 , \quad (30)$$

$$\emptyset_2 = 0.877(1 - 2\emptyset_1) , \quad (31)$$

in which χ is an empirical parameter related to the leaf angle distribution. Dai et al (2004) pointed that in case of ϕ_1=0 or ϕ_2=0, equation (29) is invalid and instead the followings should be used:

$$\bar{\mu} = \frac{1}{0.877}, \ if \ \emptyset_1 = 0 ; \quad (32)$$

$$\bar{\mu} = \frac{1}{2\emptyset_1}, \quad if \ \emptyset_2 = 0 . \quad (33)$$

In fact, χ=0 for spherical distribution. Then ϕ_1=0.5, ϕ_2=0, and $\bar{\mu}$=1. Therefore, Forest-CEW used the constant 1 for $\bar{\mu}$ and introduces a structural correction factor to adjust emissivity for a non-spherical distribution.

The net IR absorptions by leaf and stem are calculated from the down IR above a plant and the upward IR below it by

$$I_{iru} = \varepsilon_u \varepsilon_s \sigma T_s^4 + \varepsilon_u (1 - \varepsilon_s) I_{ir}^{\uparrow} + \varepsilon_l I_{ir}^{\downarrow} - 2\varepsilon_u \sigma T_u^4 , \quad (34)$$

$$I_{irs} = \varepsilon_s \varepsilon_u \sigma T_u^4 + \varepsilon_s I_{ir}^{\uparrow} + \varepsilon_s (1 - \varepsilon_l) I_{ir}^{\downarrow} - 2\varepsilon_s \sigma T_s^4 . \quad (35)$$

These equations indicate a two-layer structure for plant, i.e., a foliage layer on top of a stem layer. Although not explicitly stated by Pollard and Thompson (1995), their method includes the same implication.

The transmitted IR through tree or shrub are

$$I_{irp}^{\downarrow} = (1 - \varepsilon_u - \varepsilon_s + \varepsilon_u \varepsilon_s) I_{ir}^{\downarrow} + \varepsilon_s \sigma T_s^4 , \quad (36)$$

$$I_{irp}^{\uparrow} = (1 - \varepsilon_u - \varepsilon_s + \varepsilon_u \varepsilon_s) I_{ir}^{\uparrow} + \varepsilon_u \sigma T_u^4 . \quad (37)$$

The $I_{ir}^{\downarrow}$ is the measured IR above the canopy for a tree. The $I_{ir}^{\uparrow}$ is the emitted IR from the ground for a shrub or for a tree when shrub is not included in a simulation, i.e.,

$$I_{ir}^{\downarrow} = I_{ira} = LR + 0.54SR , \quad (38)$$

$$I_{ir}^{\uparrow} = \sigma T_g^4 . \quad (39)$$

If a simulation includes shrub, the $I_{ir}^{\uparrow}$ for a tree is calculated by parameters and temperatures of shrub objects:

$$I_{ir}^{\uparrow} = (1 - \varepsilon_u)(1 - \varepsilon_s)\sigma T_g^4 + \varepsilon_u \sigma T_u^4 + (1 - \varepsilon_u)\varepsilon_s \sigma T_s^4 . \quad (40)$$

And the $I_{ir}^{\downarrow}$ for shrub is calculated by using parameters and temperatures of tree objects:

$$I_{ir}^{\downarrow} = (1-\varepsilon_u)(1-\varepsilon_s)I_{ira} + (1-\varepsilon_s)\varepsilon_u \sigma T_u^4 + \varepsilon_s \sigma T_s^4 \ . \tag{41}$$

The $I_{ir}^{\downarrow}$ for the ground is calculated by using parameters and temperatures of tree or shrub objects, depending on whether shrub is included in a simulation:

$$I_{ir}^{\downarrow} = (1-\varepsilon_u)(1-\varepsilon_s)I_{irp}^{\downarrow} + (1-\varepsilon_s)\varepsilon_u \sigma T_u^4 + \varepsilon_s \sigma T_s^4 . \tag{42}$$

And the ground absorption of IR is

$$I_{ir} = I_{ir}^{\downarrow} - \sigma T_g^4 \ . \tag{43}$$

3.3 Energy balance

Having determined the net absorption of radiation, the temperatures of foliage or stem can be computed by

$$(c_o + c_w)\frac{\partial T}{\partial t} = I_{vis} + I_{ir} - H - LE \ . \tag{44}$$

The sensible heat flux from foliage or stem to the air in plant space is determined by the temperature gradient:

$$H = 2\Lambda \rho c_p g_h \left(T - T_p\right) . \tag{45}$$

The latent heat flux for leaves includes energy loss due to evaporation and evapotranspiration:

$$LE = 2\Lambda f_{wet} \lambda \rho g_v (q_s - q_p) + 2\Lambda(1 - f_{wet}) f_{str} \lambda \rho \frac{g_v g_s (q_s - q_p)}{g_v + g_s} . \tag{46}$$

The expression for the wet fraction of foliage or stem will be given later. The second term is not included for stem.

The net sensible heat fluxes to the air at z_p determine the air temperature in plant space:

$$c_p \frac{\partial T}{\partial t} = H_{lo} + H_u + H_s - H_{hi} \ . \tag{47}$$

As the specific heat capacity of air is small comparing to the magnitude of sensible heat fluxes, the left side of equation (47) can be omitted; therefore,

$$H_{hi} = H_{lo} + H_u + H_s \ . \tag{48}$$

Combing this and equation (45) gives

$$T_p = \frac{g_{hi} T_{hi} + g_{lo} T_{lo} + 2LAI g_{hu} T_u + 2SAI g_{hs} T_s}{g_{hi} + g_{lo} + 2LAI g_{hu} + 2SAI g_{hs}} \tag{49}$$

4 Water

Water evaporation or vapor condensation occurs on the surface of an object when the air humidity does not equal the saturated humidity on the surface. When $q_s > q_p$, the evaporation rate is estimated by

$$EV = f_{wet} 2\Lambda \rho g_v (q_s - q_p) \ . \quad (50)$$

The fraction of wet surface is the ratio of water content on the surface to the maximum amount of water that the surface can withhold:

$$f_{wet} = \frac{W_{wet}}{W_{max}} \ . \quad (51)$$

Assuming δ_w being the thickness of water film on the surface, then

$$W_{max} = 2\Lambda \delta_w \rho_w \ . \quad (52)$$

When $q_p > q_s$, the condensation rate can be calculated by

$$EC = (1 - f_{wet}) 2\Lambda \rho g_v (q_p - q_s) \ . \quad (53)$$

Evapotranspiration is assumed to occur only on leaf surface and the rate can be estimated by

$$ET = f_{str}(1 - f_{wet}) 2LAI\rho \frac{g_v g_s (q_s - q_p)}{g_v + g_s} \ . \quad (54)$$

The expression for the water stress factor f_{str} will be given in the soil section.

During a rainy period, the surface of an object intercepts water at the following rate:

$$B_w = f_{prec}(1 - e^{-0.5\Lambda \cdot PAI}) \ Prec \ . \quad (55)$$

Comparing with the LXS model, Forest-CEW multiplies LAI or SAI by PAI to obtain the effective LAI or LAI and introduces a structural correction factor to adjust the interception coefficient. For a shrub or the ground surface, the precipitation is the un-intercepted precipitation plus the dripping from the tree or shrub, i.e.,

$$Rain = Prec - B_w + \frac{W_{wet}}{86400 r_{drip}} \ . \quad (56)$$

5 Soil

Forest-CEW uses a simple soil model to simulate the transport of water and energy between soil layers. By default, the soil is divided into 8 layers with thickness of 0.05 m, 0.1 m, 0.2 m, 0.4 m, 0.8 m, 1.6 m, 3.2 m, and 6.4 m, respectively. This configuration is similar to that of Bonan (1996). Users can change the number of layers and the thickness of each layer through the parameter file for soil.

The exchange of heat and vapor on the surface is treated similarly to the process on leaf or stem surface. But a virtual water pool is set aside for the interception of rain water. If the water contents in the surface layer is smaller than its capacity, which is set to 90% of porosity, rain water infiltrate into the layer; otherwise rain water will be detained by the pool temporally.

Between any two layers, the exchange rate of water is computed by

$$J_w = -K(\psi_m)\frac{d\psi_m}{dz} - gK(\psi_m)\,, \tag{57}$$

$$\psi_m = \psi_s\left(\frac{\theta}{\theta_s}\right)^{-b}, \tag{58}$$

$$K(\psi_m) = K_s\left(\frac{\theta}{\theta_s}\right)^{2b+3}. \tag{59}$$

And the exchange of heat by

$$J_h = g_{soi}\frac{dT}{dz}\,, \tag{60}$$

$$g_{soi} = f_{scp}\frac{1.75 f_{sa} g_{sa} + 0.92 f_{sw} g_{sw} + 0.54 f_{sm} g_{sm}}{1.75 f_{sa} + 0.92 f_{sw} + 0.54 f_{sm}} \tag{61}$$

In contrast to the method Campbell and Norman (1998), Forest-CEW uses constant correction factors for the conductance of air, water, and mineral; and introduces a structural correction factor to count for unknown properties of the soil. The constant values are used by Santos and Costa (2004).

The equation of the volumetric heat capacity of soil also includes a structural factor f_{scv}:

$$c_{soi} = f_{scv}\frac{f_{so}c_{vo} + f_{sw}c_{vw} + f_{sm}c_{vm}}{f_{so} + f_{sw} + f_{sm}}\,. \tag{62}$$

The water stress factor in the equations of evapotranspiration and photosynthesis is calculated by

$$f_{str} = \frac{1 - e^{-c_{str}AWI}}{1 - e^{-c_{str}}}\,. \tag{63}$$

The available water indicator AWI is related to the root profile and water contents in the soil:

$$AWC = \sum_i f_{root}(i)\delta(i) \tag{64}$$

$$\delta(i) = \begin{cases} 1, & water\ content > wilting\ point \\ 0, & water\ content < wilting\ point \end{cases} \tag{65}$$

The mass of roots is assumed to decrease exponentially with depth:

$$f_{root}(z) = \frac{e^{-c_r z}}{\int e^{-c_r z} dz}\,, \tag{66}$$

$$c_r = -ln(0.01)/z_r. \tag{67}$$

These equations indicate that the root mass per unit thickness at depth z_r decreases to 1% of the total mass.

6 Photosynthesis

Forest-CEW implements the Farquhar–von Caemmerer–Berry model (Farquhar et al., 1980; Collatz et al., 1991; Dubois et al., 2007) to simulate photosynthesis. The gross rate is the smallest of the light-limited assimilation rate J_e and the Rubisco-limited rate J_c:

$$A = min\begin{Bmatrix} J_e \\ J_c \end{Bmatrix}, \tag{68}$$

$$J_e = \frac{J_m(C_i - \Gamma^*)}{C_i + 2\Gamma^*}, \tag{69}$$

$$J_c = \frac{V_m(C_i - \Gamma^*)}{C_i + K_c(1 + \frac{C_o}{K_o})}, \tag{70}$$

$$\Gamma^* = \frac{500 C_o}{\tau}, \tag{71}$$

The whole chain electron transport rate J_m is proportional to the absorbed PPFD in Campbell and Normman (1998), but was expressed as a function of the maximum rate J_{max} and PPFD by Farquhar and Caemmerer (1982):

$$J_m = \frac{J_{max} PPFD}{PPFD + q_n J_{max}}, \tag{72}$$

This imposes a photoinhibition (Long et al., 1994) effect at high PPFD values. Forest-CEW uses the same equation of the CANOAK model (Baldocchi and Harley, 1995):

$$J_m = \frac{J_{max} PPFD}{\sqrt{PPFD^2 + {q_c}^2 {J_{max}}^2}}, \tag{73}$$

Forest-CEW also adopts the Boltzmann function the CANOAK model to express the dependency of V_m on temperature:

$$V_m = V_{max} \frac{E_p exp(\frac{E_v(T_u - T_{opt})}{RT_{opt}T_u})}{E_p - E_v(1 - exp(\frac{E_p(T_u - T_{opt})}{RT_{opt}T_u}))}, \tag{74}$$

and constants for the Arrhenius equations of τ, Kc, and Ko:

$$\tau = 2904.12 exp(\frac{-29.0(T_u - 298)}{298 R T_u}), \tag{75}$$

$$K_c = 274.6 exp(\frac{80.5(T_u - 298)}{298 R T_u}), \tag{76}$$

$$K_o = 419.8exp(\frac{14.5(T_u-298)}{298RT_u}) , \quad (77)$$

As equation (68) produces discrete values, the gross rate is calculated by the following colimit functions:

$$A = \frac{J_e+J_c-\sqrt{(J_e+J_c)^2-4\times0.95J_eJ_c}}{2\times0.95} , \quad (78)$$

The intercellular CO2 concentration (C_i) cannot be measured directly. Forest-CEW estimates it by the same iteration method of Zeng et al. (2017), which used the relations between the gross rate and the CO2 fluxes from air to leaf surface and into the cells, i.e.,

$$A = \frac{\rho}{m_w} g_v(CO_2 - C_s) , \quad (79)$$

$$A = \frac{\rho}{m_w}\frac{g_s g_v}{g_s+g_v}(CO_2 - C_i) . \quad (80)$$

Two models for estimating the stomatal conductance g_s are included in Forest-CEW. One uses the dependence of g_s on the saturated relative humidity (Ball et al., 1987):

$$g_s = g_0 + g_1\frac{h_s A}{C_s} . \quad (81)$$

Another uses the dependence on VPD (Leuning, 1995):

$$g_s = g_0 + \frac{g_1}{1+g_{vpd}VPD}\frac{A}{C_s} . \quad (82)$$

The dark respiration of leaves is simulated by the Arrhenius equation that includes the regulation of the respiration by PPFD

$$R_d = \frac{R_{d25}exp(\frac{E_d(T_u-298)}{298RT_u})}{1+0.001PPFD} . \quad (83)$$

This equation suppresses the respiration by about 50% at high PPFDs (Villar et al., 1995)

The temperature dependency of respirations of stem and roots and the decomposition of litters take the form of

$$R_e = R_{e25}exp(\frac{E_d(T_u-298)}{298RT_u}) . \quad (84)$$

The decomposition of dead root is also affected by the moisture factor of the soil (Walse et al. 1998), which is calculated by

$$R_e = \frac{\theta^{pw}}{k_w+\theta^{pw}} . \quad (85)$$

7 Static and dynamic mode

In a static mode simulation, the carbon storages of stem, roots, and litters remain constant; and leaf carbon is calculated from LAI and specific leaf are SLA as

$$C_u = LAI/SLA\ . \tag{86}$$

In a dynamic mode simulation, the net increase of carbon by photosynthesis is allocated to leave, stem, and roots by constant fractions. Litter carbons also increase due to leaf fall and stem death. The aged fine root become coarse root and the dead coarse root joins the dead organic carbon in the soil. These processes are parameterized by residence time rt as

$$\Delta C = C(1 - e^{-k_t \Delta t})\ , \tag{87}$$

$$k_t = -\frac{ln(0.01)}{rt}. \tag{88}$$

Equation (86-87) indicate that a carbon storage reduces to 1% of the initial value after rt.

8 Simulation

Forest-CEW integrates model equations using the forward Euler method in two steps. The first step estimates all fluxes at time t by the values of state variables of the same time. The second step updates state variables to have the values at t+tΔ. In the initial stage, state variables are set to have the values or derived values of the first input data, or reloaded from a previous simulation.

We have chosen the method as it gives the maximal flexibility to change model configuration. Our experiments have shown that the outcome does not vary significantly as long the time step is much smaller than 1 hour. Considering the uncertainty of many assumptions in such a model, the effect of model performance by the precision of the numerical integration is small.

Table 1 List of variables and parameters. Equations often use subscripts of u for foliage or leaf, s for stem, p for plant, g for ground, soi for soil, ir for long wave radiation, and vis for visible light radiation.

Symbol	Units	Default Value	Remark
A	μmol m^{-2} s^{-1}		Gross photosynthesis rate
AWI			Available water indicator
b		6.6	Parameter of moisture release equation
B_w	mm hr^{-1}		Water interception rate
c_p	J kg^{-1} K^{-1}	1.01e3	Specific heat capacity of air
c_o	J kg^{-1} K^{-1}	1.92e3	Specific heat capacity of dry organic matter
c_w	J kg^{-1} K^{-1}	4.18e3e3	Specific heat capacity of water
c_{vo}	J kg^{-1} K^{-1}		Volumetric heat capacity of dry organic matter
c_{vw}	J kg^{-1} K^{-1}		Volumetric heat capacity of water
c_{vm}	J kg^{-1} K^{-1}		Volumetric heat capacity of water
c_{str}		-5.0	Water stress coefficient
C_O	mmol mol^{-1}	210	Atmospheric oxygen concentration.
CO_2	μmol mol^{-1}		Atmospheric carbon dioxide concentration
C_i	μmol mol^{-1}		Intercellular CO2 concentration
C_s	μmol mol^{-1}		CO2 concentration on leaf surface
d	m	0.1	Typical leaf width or stem size.
E_v	KJ mol^{-1}	55	Activation energy for carboxylation
E_p	KJ mol^{-1}	220	Enthalpy term of the Boltzmann function
E_r	KJ mol^{-1}	38	Activation energy for dark respiration
EC	kg m^{-2} s^{-1}		Water condensation
EV	kg m^{-2} s^{-1}		Water evaporation
ET	kg m^{-2} s^{-1}		Water evapotranspiration
f_{scp}		1.0	Structural factor for soil heat conductivity equation
f_{scv}		1.0	Structural factor for soil heat capacity equation
f_{prec}		1.0	Structural factor for rain water interception
f_{sa}			Volume fraction of air in soil
f_{sw}			Volume fraction of water in soil
f_{sm}			Volume fraction of mineral in soil
f_{so}			Volume fraction of organic matter in soil
f_{em}		1.0	Structural correction factor for emissivity
f_{wet}			Fraction of wet leaf or stem
f_{str}			Water stress factor
f_{root}			Fraction of root in a soil layer
f_w			Factor of soil water content affecting decomposition.
g	m s^{-2}	9.8	Gravity
g_h	m s^{-1}		Heat conductance of leaf or stem surface
g_{hu}	m s^{-1}		Heat conductance of leaf surface
g_{hs}	m s^{-1}		Heat conductance of stem surface
g_v	m s^{-1}		Vapor conductance of leaf or stem surface
g_H	m s^{-1}		Conductance of heat between airs
g_V	m s^{-1}		Conductance of vapor between airs
g_s	mol m^{-2} s^{-1}		Stomatal conductance of gas
g_0	mol m^{-2} s^{-1}	0.003	Minimal stomatal conductance of gas
g_1		5.6	Sensitivity coefficient of g_s
g_{vpd}	kPa^{-1}	1.0	VPD coefficient of g_s
H	W m^{-2}		Sensible heat flux
H_u	W m^{-2}		Sensible heat flux from foliage to air
H_s	W m^{-2}		Sensible heat flux from stem to air
H_{lo}	W m^{-2}		Sensible heat flux from lower air
H_{hi}	W m^{-2}		Sensible heat flux to higher air
I_{vis}	W m^{-2}		Visible light radiation
I_{ir}	W m^{-2}		Long wave radiation

J_c	μmol m^{-2} s^{-1}		Photosynthesis rate imposed by light
J_e	μmol m^{-2} s^{-1}		Photosynthesis rate imposed by Rubisco
J_{max}	μmol m^{-2} s^{-1}	80	Maximum rate of whole chain electron transport
J_m	μmol m^{-2} s^{-1}		Rate of whole chain electron transport
J_h	W m^{-2}		Heat exchange rate between soil layers
J_w	kg m^{-2} m^{-2}		Water exchange rate between soil layers
k_c	$°C^{-1}$		Temperature coefficient for respiration and decomposition
K_c	μmol mol^{-1}		Michaelis-Menten constant of Rubisco for CO_2
K_o	mmol mol^{-1}		Michaelis-Menten constant of Rubisco for O_2
K_s	kg s m^{-3}	4.2e-5	Saturation hydraulic conductivity
k_w		0.1	Soil water content coefficient for decomposition
H	W m^{-2}		Sensible heat flux from object to air or from low air to high are
LAI	m^2 m^{-2}		Leaf area index
LE	W m^{-2}		Latent heat flux
LR	W m^{-2}		Downward long wave radiation
l_m	m		Mean distance between leaves
m_a	kg mol^{-1}	0.028964	Air mass
m_w	kg mol^{-1}	0.018016	Water mass
p_w		2.0	Soil water content exponential coefficient for decomposition
P	kPa		Atmospheric pressure
PAI	m^2 m^{-2}		Plant area index
PPFD	μmol m^{-2} s^{-1}		Photosynthetic photon flux density
Prec	mm hr^{-1}		Precipitation
q_n		7	Quantum yield coefficient
q_s	Kg kg^{-1}		Saturated humidity
q_p	Kg kg^{-1}		Humidity at z_p
r_{drip}	day	1	Dripping time of surface water
r_{c0}	μmol kg^{-1} s^{-1}	0.5	Respiration rate at 0°C
rt	yr		Residence time of leaf, stem, or root
R	KJ $mole^{-1}$ K^{-1}	0.008314	Gas constant
R_d	μmol m^{-2} s^{-1}		Dark respiration rate of leaf
R_{d25}	μmol m^{-2} s^{-1}		Dark respiration rate of leaf at 25°C
R_e	μmol kgC^{-1} s^{-1}		Respiration rate
R_{e25}	μmol kgC^{-1} s^{-1}		Respiration rate at 25°C
SAI	m^2 m^{-2}		Stem area index
SR	W m^{-2}		Global solar radiation
t	S		Time
T_a	°C		Air temperature above canopy
T_d	°C		Deep soil temperature
T_p	K		Air temperature at z_p
T	K		Temperature
T_u	K		Leaf temperature
T_s	K		Stem temperature
T_g	K		Ground temperature
T_{opt}	K	311	Peak leaf temperature for V_{max}
TC	°C		Temperature
U	m s^{-1}		Wind speed
u^*	m s^{-1}		Friction velocity
u_{top}	m s^{-1}		Wind speed at z_{top}
u_{ref}	m s^{-1}		Wind speed at z_{ref}
V_{max}	μmol m^{-2} s^{-1}	75	Maximum Rubisco capacity per unit leaf area
V_m	μmol m^{-2} s^{-1}		Rubisco capacity per unit leaf area
VPD	kPa		Vapor pressure deficit
W	kg m^{-2}		Water content
W_{wet}	kg m^{-2}		Water content on wet surface
W_d	m^3 m^{-3}		Deep soil water content
z_{ref}	m		Reference height
z_{top}	m		Height of foliage top

z_{bot}	m		Height of foliage bottom
z_p	m		Characteristic height of foliage
z_d	m		Zero plane displacement
z_m	m		Roughness length for momentum
z_h	m		Roughness length for heat
z_v	m		Roughness length for vapor
z_r	m	3.0	Root profile parameter
α		0.13	Reflectivity (the default value is for leaves)
β		0.8	Absorptivity (the default value is for leaves)
Λ	$m^2\ m^{-2}$		Generic symbol for LAI and SAI
ε			Emissivity or absorptivity of long wave radiation leaves
Γ^*	$\mu mol\ mol^{-1}$		Compensation point of CO2 concentration
κ		0.4	von Karman constant
λ	$J\ kg^{-1}$	2.2647e6	Latent heat of vaporization of water
ϕ_M			Diabatic correction factor for momentum
ϕ_H			Diabatic correction factor for heat
ψ_m	$J\ kg^{-1}$		Matric water potentials
ψ_s	$J\ kg^{-1}$		Air entry water potential
ρ	$kg\ m^{-3}$		Air density
ρ_w	$kg\ m^{-3}$	999.8	Water density
σ	$W\ m^{-2}\ K^{-4}$	5.6697e-8	Stefan-Boltzmann constant
θ	$m^3\ m^{-3}$		Water content
θ_s	$m^3\ m^{-3}$		Saturated water content
δ_w	m	0.001	Thickness of water film
τ			Specific ratio of CO_2/O_2
ξ			Stability indicator
χ			Empirical parameter of leaf angle distribution

Reference

Baldocchi, D.D. and P.C. Harley, 1995. Scaling carbon dioxide and water vapor exchange from leaf to canopy in a deciduous forest: model testing and application. Plant, Cell and Environment. 18: 1157-1173.

Baldocchi, D.D. and K.B.Wilson, 2001. Modeling CO2 and water vapor exchange of a temperate broadleaved forest across hourly to decadal time scales. Ecological Modeling. 142: 155-184.

Ball, J.T., J.T. Woodrow, and J.A. Berry, 1987. A model predicting stomatal conductance and its contribution to the control of photosynthesis under different environmental conditions. In: Biggins J ed. Progress in Photosynthesis Research, Vol. 4. Proceedings of the 7th International Congress on Photosynthesis. Matins Nijhoff, Dordrecht, the Netherlands. 221–224.

Blyth, E.M., R.J. Harding, and R. Essery, 1999. A coupled dual source GCM SVAT. Hydrology and Earth System Sciences Discussions, European Geosciences Union, 3 (1):71-84.

Bonan, G. B., 1996. A land surface model (LSM version 1.0) for ecological, hydrological, and atmospheric studies: Technical description and user's guide. NCAR Technical Note. NCAR/TN-417+STR. P150.

Campbell G.S.and J.M. Norman, 1998, An introduction to environmental biophysics. Second Edition. Springer-Verlag New York, Inc.

Dai, Y., R.E. Dickinson, and Y.P.Wang, 2014. A Two-Big-Leaf Model for Canopy Temperature, Photosynthesis, and Stomatal Conductance. Journal of Climate, 17: 2281-2299.

Dickinson, R. E., 1983: Land surface processes and climate-surface albedos and energy balance. Advances in Geophysics, Vol. 25, Academic Press, 305–353.

Farquhar, G.D., S. von Caemmerer, and J.A. Berry, 1980. A biochemical model of photosynthetic CO2 assimilation in leaves of C3 species. Planta, 149, 78–90.

Farquhar G.D. and S. von Caemmerer, 1982. Modeling photosynthetic response to environmental conditions. In Encyclopedia of Plant Physiology 12B. (eds O.L. Lange et al.) pps. 549-587. Springer-Verlag, Berlin.

Leuning, R., 1995. A critical appraisal of a coupled stomatal–photosynthesis model for C3 plants. Plant, Cell and Environment, 18: 339–357.

Long, S.P., S. Humphries, and P.G. Falkowski, 1994. Photoinhibition of photosynthesis in nature. Annu. Rev. Plant Physial. Plant Mol. BioI., 45:633-62.

Medlyn, B.E., R.A. Duursma, , D. Eamus, D.S. Ellsworth, I.C. Prentice, C.V.M. Barton, K.Y. Crous, P. De Angelis, M. Freeman, and L. Wingate, 2011. Reconciling the optimal and empirical approaches to modelling stomatal conductance. Global Change Biol., 17:2134–2144.

Pollard, D. and S.L. Thompson, 1995. The effect of doubling stomatal resistance in a global climate model. Global Planet. Change 10, 129–161.

Santos, S. N. M. and M.H. Costa, 2004. A simple tropical ecosystem model of carbon, water and energy fluxes. Ecological Modelling. 176: 291–312. doi:10.1016/j.ecolmodel.2003.10.032.

Sellers, P.J., D.A. Randall, G.J. Collatz, J.A. Berry, C.B. Field, D.A. Dazlich, C. Zhang, G.D. Collelo, and L. Bounoua, 1996. A Revised Land Surface Parameterization (SiB2) for Atmospheric GCMS. Part I: Model Formulation. Journal of Climate. 9: 676-705.

TAN Zheng-Hong, ZENG Jiye, LIU Shu-Guang, PENG Shu-Shi, ZHU Biao, XU Xiang-Tao, WU Zhi-Xiang, LI Yi-De, SONG Liang, ZHAO Jun-Fu, ZHANG Xiang, ZHANG Yong-Jiang, SAIGUSA Nobuko, SONG Qing-Hai, YAN Wen-De, and YANG Lian-Yan. 2018. Forest-CEW: A model for carbon-energy-water process in forest ecosystems. (to be submitted)

Villar, R., A. A. Held, and J. Merino, 1995. Dark leaf respiration in light and darkness of an evergreen and a deciduous plant species. Plant Physiol. 107: 421-427.

Walse, C., B. Berg, and H. Sverdrup, 1998. Review and synthesis of experimental data on organic matter decomposition with respect to the effect of temperature, moisture, and acidity. Envorn. Rev. 6:25-40.

Zeng, J., Z.H. Tan, and N. Saigusa, 2017. Using approximate Bayesian computation to infer photosynthesis model parameters. Chinese Journal of Plant Ecology, 41, 378–385. doi: 10.17521/cjpe.2016.0067